frontiers in Earth Science

ORIGINAL RESEARCH
published: 15 November 2021
doi: 10.3389/feart.2021.754137

New Detrital Apatite Fission Track Thermochronological Constraints on the Meso-Cenozoic Tectono-Thermal Evolution of the Micangshan-Dabashan Tectonic Belt, Central China

Tao Tian[1,2], *Peng Yang*[3]*, *Jianming Yao*[2], *Zhonghui Duan*[2], *Zhanli Ren*[3], *Deliang Fu*[1,2] *and Fu Yang*[1,2]

[1]Key Lab of Coal Resources Exploration and Comprehensive Utilization, MNR, Xi'an, China, [2]Shaanxi Coal Geology Group Co., Ltd., Xi'an, China, [3]State Key Laboratory of Continental Dynamics, Department of Geology, Northwest University, Xi'an, China

OPEN ACCESS

Edited by:
Xuhua Shi,
Zhejiang University, China

Reviewed by:
Jingxing Yu,
Institute of Geology, China
Yuntao Tian,
Sun Yat-sen University, China

***Correspondence:**
Peng Yang
p.yang@nwu.edu.cn

Specialty section:
This article was submitted to Structural Geology and Tectonics, a section of the journal Frontiers in Earth Science

Received: 06 August 2021
Accepted: 14 October 2021
Published: 15 November 2021

Citation:
Tian T, Yang P, Yao J, Duan Z, Ren Z, Fu D and Yang F (2021) New Detrital Apatite Fission Track Thermochronological Constraints on the Meso-Cenozoic Tectono-Thermal Evolution of the Micangshan-Dabashan Tectonic Belt, Central China. Front. Earth Sci. 9:754137. doi: 10.3389/feart.2021.754137

The Micangshan-Dabashan tectonic belt, located in the southern Qinling-Dabie Orogen near the northeastern Tibetan Plateau, is a crucial area for understanding the processes and mechanisms of orogenesis. Previous studies have been focused on the cooling process via thermochronology and the mechanism and process of basement uplift have been investigated. However, the coupling process of basement exhumation and sedimentary cap cooling is unclear. The tectono-thermal history constrained by the detrital apatite fission track (AFT) results could provide valuable information for understanding crustal evolution and the coupling process. In this study, we provided new detrital AFT thermochronology results from the Micangshan-Dabashan tectonic belt and obtained nine high-quality tectono-thermal models revealing the Meso-Cenozoic cooling histories. The AFT ages and lengths suggest that the cooling events in the Micangshan area were gradual from north (N) to south (S) and different uplift occurred on both sides of Micangshan massif. The cooling in Dabashan tectonic zone was gradual from northeast (NS) to southwest (SW). The thermal histories show that a relatively rapid cooling since ca. 160 Ma occurred in the Micangshan-Dabashan tectonic belt, which was a response to the event of Qinling orogenic belt entered the intracontinental orogenic deformation. This cooling event may relate to the northeastward dextral compression of the Yangtze Block. The sedimentary cap of Cambriano-Ordovician strata responded positively to this rapid cooling event and entered the PAZ since ca. 63 Ma. The deep buried samples may be limited affected by climate and water erosion and the accelerated cooling was not obvious in the Late Cenozoic. Collectively, the cooling processes of basement and sedimentary cap in Micangshan-Dabashan tectonic belt were inconsistent. The uplift of the sedimentary area is not completely consistent with that of the basement under thrust and nappe action. The rigid basement was not always continuous and rapidly uplifted or mainly showed as lateral migration in a certain stage because of the different intensities and

modes of thrust and nappe action, and the plastic sedimentary strata rapidly uplifted due to intense folding deformation.

Keywords: detrital apatite fission track, tectono-thermal evolution, differential uplifting, basin-mountain coupling, Micangshan-Dabashan belt

INTRODUCTION

The Micangshan-Dabashan tectonic belt, located at the northeastern margin of the Tibetan Plateau, is a key "basin-mountain coupling" transitional orogenic belt that separates the Qinling orogenic belt to the north and the Sichuan Basin to the south (**Figure 1**). Its tectonic evolution and thermal histories have attracted much attention due to its relevance in understanding the onset of the Asian monsoon, drainage adjustment of the Yangtze River system, growth of the Tibetan Plateau, evolution of the Qinling-Dabie Orogen, erosional lowering of the Sichuan Basin as well as for evaluating the new Frontier exploration potential of lower Cambrian and Neoproterozoic hydrocarbon reservoirs (including shale gas) (Clark et al., 2004; Enkelmann et al., 2006; Shen et al., 2007; Richardson et al., 2008; Tian et al., 2010; Tian et al., 2012; Yang et al., 2013; Yang et al., 2017). The

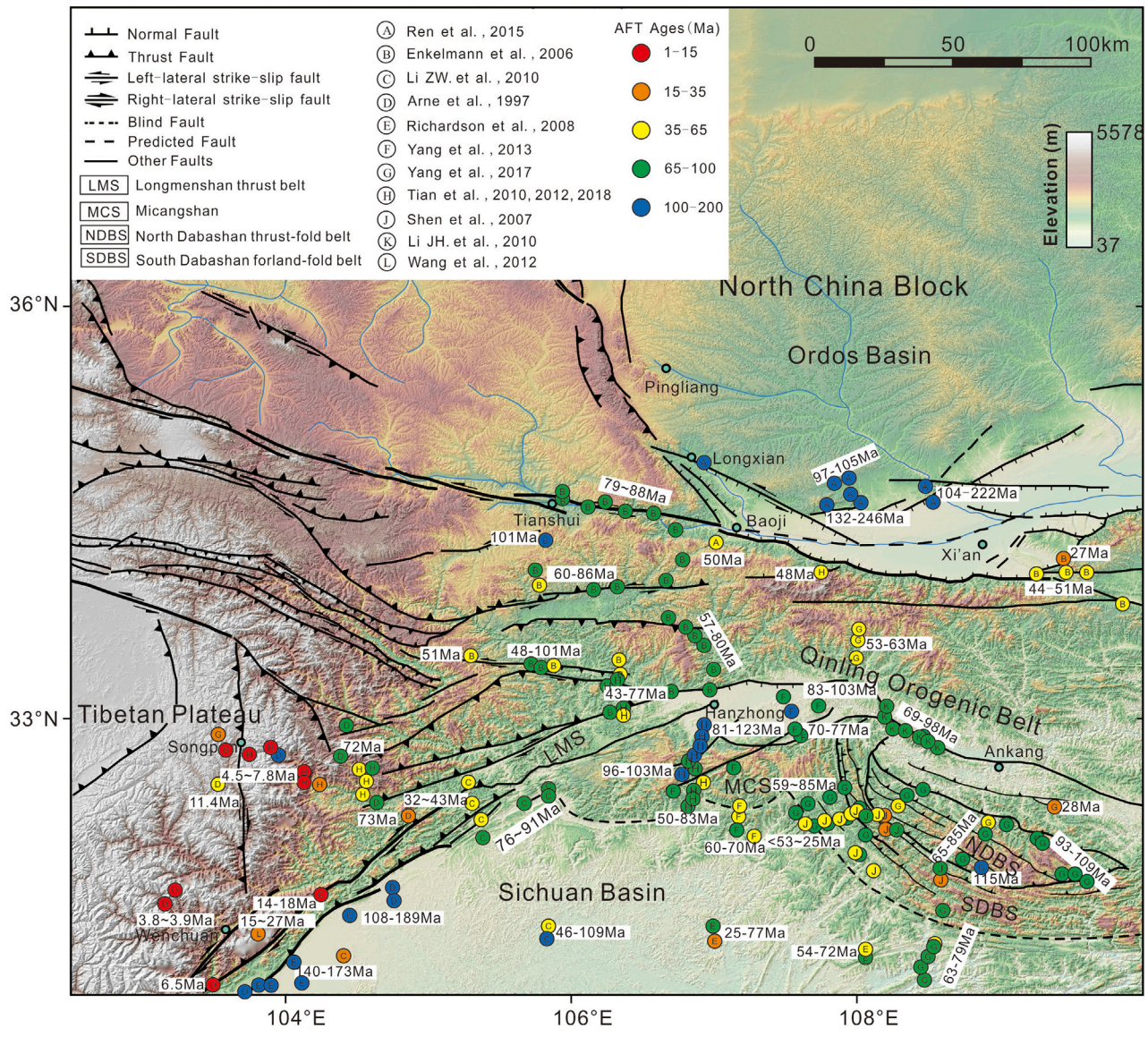

FIGURE 1 | Published apatite fission track (AFT) ages (in Ma) plotted on geologic-tectonic maps of the Micangshan, Dabashan and adjacent regions; different ages are noted in different colours.

Micangshan-Dabashan tectonic belt formed after collision with the South China Block (SCB) and North China Block (NCB) in the Indochina period and intracontinental orogeny in the Yanshanian-Himalayan period (Zhang et al., 1989; Meng and Zhang, 2000; Meng et al., 2005; Tan et al., 2007; Xu et al., 2009; Tian et al., 2010; Tian et al., 2012). The internal structure is complex, and the deformation characteristics are obviously different among different units. The tectono-thermal evolutionary histories need to be addressed in a timely manner, especially given that the evolution of the Micangshan-Dabashan tectonic belt since the Meso-Cenozoic has remained controversial.

As one of the most important thermochronological methods, apatite fission track (AFT) parameters provide quantitative information on cooling and record the thermal history of rocks (Green et al., 1986; Green, 1988; Gallagher, 2003), and these parameters are typically interpreted as a result of surface uplift and erosion (Tian et al., 2010; Tian et al., 2012; Tian et al., 2013; Lei et al., 2012; Ren et al., 2015; Qi et al., 2016; Powell et al., 2017; Tian et al., 2018). Previous work that has focused on the thermal history derived from a variety of thermochronometry dating methods, such as U-Pb, $^{40}Ar/^{39}Ar$, (U-Th)/He and AFT, in the Longmenshan, Micangshan and Dabashan areas has been published, and the dating methods and results have mainly been applied to investigate the cooling events and the coupling process of the Tibetan Plateau uplift (Arne et al., 1997; Enkelmann et al., 2006; Shen et al., 2007; Richardson et al., 2008; Li ZW et al., 2010; Li ZW et al., 2012; Li JH et al., 2010; Li et al., 2011; Chang et al., 2010; Tian et al., 2010; Tian et al., 2012; Tian et al., 2013; Tian et al., 2016; Tian YT et al., 2018; Yang et al., 2013; Yang et al., 2017; Shen et al., 2019). The thermochronometry dating and thermal histories results above and others from the, Tongbai-Dabieshan (Webb et al., 1999; Reiners et al., 2003; Hu et al., 2006), Taibaishan (Wang et al., 2005) and Western Qinling (Zheng et al., 2004; Enkelmann et al., 2006) show that the regional uplift occurred from the Late Jurassic to the Early Cretaceous and an accelerated uplift since the Late Cenozoic which related to the growth of the northeastern Tibetan Plateau. The Longmenshan tectonic defines the eastern margin of the eastern part of the Tibetan Plateauis and the western boundary of the Micangshan tectonic zone. The Longmenshan experienced multiple phases of intracontinental deformation during Mesozoic-Cenozoic (Tian et al., 2013; Tian et al., 2016; Tian YT et al., 2018; Shen et al., 2019), such as the Early Cretaceous (ca.119–131 Ma) and the Late Cenozoic (ca.30–25 Ma, 20 Ma, and 12–5 Ma, Arne et al., 1997; Kirby et al., 2002; Godard et al., 2009; Wang et al., 2012), and these tectonic activities may relate to the uplift and denudation in Micangshan tectonic zone.

Generally, the previous low-temperature thermochronological data was focused on the uplift of basement and show that the timing of the uplift in different areas of the Micangshan-Dabashan tectonic belt during the Mesozoic to Cenozoic was different. Furthermore, the apatite fission track (AFT) ages in the same area were inconsistently affected by factors such as experimental conditions and the nature of the samples (**Figure 1**). In contrast to the abundant thermochronology studies of the basement uplift, few studies have been conducted in the thermal evolution of sedimentary cap and its relationship with the uplift of basement. During the orogenic process, the uplift and denudation of the mountain were closely related to deposition in the nearby basin, which was a coupling process. The basin sediments adjacent to the orogenic belt recorded abundant uplift and denudation information during the late orogenic process. Therefore, the detrital AFT collected from the sedimentary basin could reveal its thermal history and the exhumation cooling history of the orogenic belt in the provenance area (Shen et al., 2005; Homke et al., 2010; Lin et al., 2015; Zhang et al., 2016; Du et al., 2018).

Detrital AFT analysis in the hinterland of the Micangshan and Dabashan areas is rare, and there is a lack of information regarding the tectono-thermal history of the sedimentary area. There are some differences in the results of previous thermochronometry studies related to the timing of cooling events in Micangshan and Dabashan. Therefore, new detrital AFT data and analyses need to be provided as key evidence for the timing of cooling events. In this study, we present a low-temperature thermochronology study of the Micangshan and Northern Dabashan, employing apatite fission track (AFT) data from nine detrital samples to assess the regional cooling history and providing information about the coupling relationship of uplift in basement and sedimentary areas.

GEOLOGICAL SETTING

The Micangshan-Dabashan tectonic belt is located at the junction of the Qinling orogenic belt and Sichuan Basin (**Figures 2A,B**), which was a passive continental margin in the early Paleozoic (Tian et al., 2010; Yang et al., 2013). The South China Block subducted under the North China Block beginning in the late Caledonian, underwent full collision until the Late Triassic, and experienced continuous compression and reconstruction in the Yanshan-Himalayan. Structural phenomena such as continuous fold deformation, differential uplift and thrust-slip faults are widely developed (Shi and Shi, 2014, **Figures 2C,D**).

The Dabashan tectonic belt is an important part of the multilayered thrust nappe tectonic system on the southern margin of the Qinling Orogen. The Late Triassic collision of the South Qinling and Yangtze Block along the Mianlue suture and the large-scale intracontinental subduction of the Yangtze Block beneath the Qinling Orogen during the Yanshanian period (Cheng et al., 2004; Huang and Wu, 1992) resulted in extensive fold and thrust deformation. Usually, the Dabashan tectonic belt is divided into two different tectonic units and sedimentary systems, the Southern Dabashan (SDBS) and the Northern Dabashan (NDBS), and they are bounded by the Chengkou fault (He et al., 1997; Li et al., 2011, Li et al., 2015; Yue, 1998, **Figure 2E**). The Dabashan thrust belt initiated and propagated southwards into the northern Sichuan Basin, which resulted in the formation of the Dabashan foreland basin (Wang et al., 2004). A number of NW-SE-trending faults are developed, and the Chengkou fault is the main active surface stacking the thrusts in the SW direction (Dong et al., 2006; Dong et al., 2008). The thrust belt mainly comprises Proterozoic basement and Sinian-Silurian limestone-dominated cover, which are all intruded by Silurian mafic

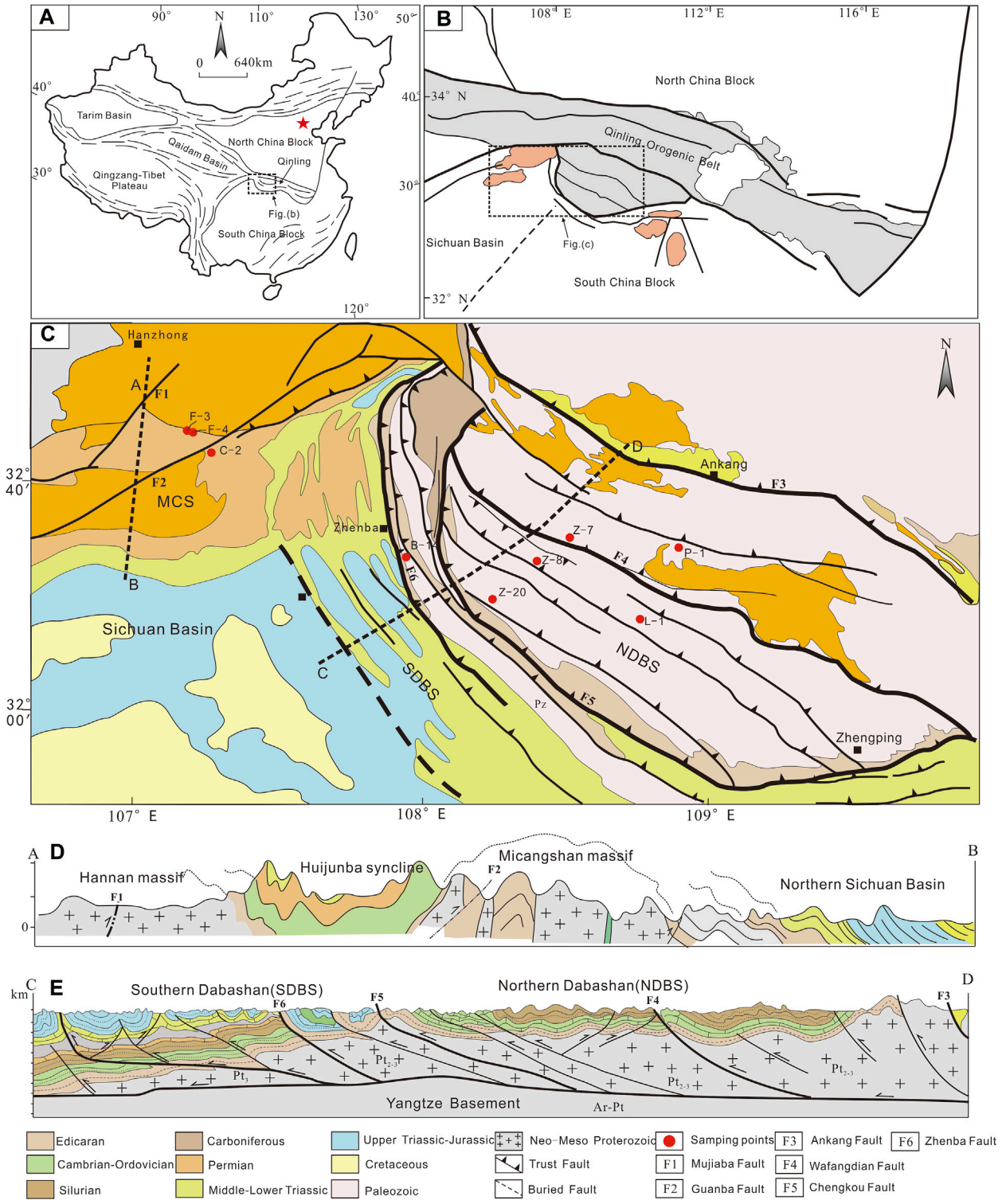

FIGURE 2 | Geological sketch map of the study area and sampling location. **(A)** The study area is located between the SCB and NCB in Central China **(B)** The Dabashan tectonic belt is on the southern margin of the Qinling Orogen. Micangshan is located between the Sichuan Basin and Qinling Orogen **(C)** Sample locations plotted on a geologic-tectonic map of the Micangshan and Dabashan tectonic belts. **(D)**, **(E)** Geologic cross-sections "A-B" and "C-D", modified from Yang et al. (2013) and Shi et al. (2012).

dikes (Zou et al., 2011; Li RX. et al., 2012). Devonian to Middle Triassic strata are exposed only north of the Ankang fault, and lower Paleozoic strata occur along faults and unconformably contact rare Lower to Middle Jurassic strata. Micangshan is located on the northwestern margin of the Upper Yangtze, adjacent to the Longmenshan tectonic belt in the west and to the Southern Dabashan foreland fold-thrust belt in the east. The main structural lines in the area spread out in the NE direction, and most of them behave similarly to thrust faults and slip faults (**Figure 2**). The intersection with the South Qinling block shows a strong dextral arc, with a nearly N-S-trending compound anticline. The Archean-early Proterozoic granitic basement and a small amount of basic intrusive rocks are exposed in the central uplift area of Micangshan, in which there are relatively intact residual synclines, mainly the Permian-Triassic system and the Sinian to Silurian system on the two wings. The overlying strata experienced deformation during the later stage. The lithology of outcrops in the regions varies after uplift and denudation (Chang et al., 2010; Li et al., 2008; Tian YT et al., 2018; Tian et al., 2019). From north to south in the Micangshan tectonic zone, a distinct succession of Neogene-Quaternary sedimentary (Hanzhong Basin), crystalline basement (Hannan and Micangshan massifs), Sinian-Triassic sedimentary (Huijunba syncline) and Sinian-Cretaceous sedimentary cover (Norther Sichuan Basin) can be identified (**Figure 2D**).

SAMPLES AND METHODS

A total of nine outcrop samples were collected for apatite fission track analysis, three of which were from the vicinity of the Huijunba syncline in the Micangshan tectonic belt, and six were from the Dabashan tectonic belt (**Figure 2C**). All the samples were from lower Cambrian to Lower-Middle Ordovician siltstone and sandstone.

Apatite was separated from each sample using standard heavy liquid and magnetic separation techniques. Apatite grains were mounted in epoxy resin on glass slides and then ground and polished to an optical finish to expose internal grain surfaces. Spontaneous fission tracks in the apatite were etched in 6.6% HNO_3 at 25°C for 30 s to reveal the spontaneous fission tracks. Low-U muscovite in close contact with these grains served as an external detector during irradiation (Yuan et al., 2003; Yuan et al., 2006). Neutron fluence was monitored in CN5 U dosimeter glasses (Bellemans et al., 1995). After irradiation in the reactor, the external muscovite detector was detached and etched in 40% HF for 20 min at room temperature to reveal induced tracks. Track densities of both spontaneous and induced fission track populations were measured with a dry objective at ×10015 magnification. Fission track ages were calculated using the IUGS-recommended zeta calibration approach (Hurford, 1990), which is shown in **Eq. 1**. Zeta values used in this study were determined from repeated measurements of standard apatites (Hurford and Green, 1983). The weighted mean zeta value for apatite used by the fission track operator was 391 ± 17.8 a/cm^2 according to the calibration of sample standards. The lengths of the horizontally confined fission tracks were measured exclusively in prismatic apatite crystals because of the anisotropy of annealing of fission tracks in apatite (Green et al., 1986).

$$T_{\text{sample}} = \frac{1}{\lambda_d}\ln\left(1 + \lambda_d \xi \frac{\rho_s}{\rho_i}\rho_d\right) \quad (1)$$

where T_{sample} is the AFT age of the samples; λ_d, which is 1.55125 × 10^{-10}a^{-1}, is the decay constant of ^{238}U; ρ_s is the track density for spontaneous fission tracks; ρ_i is the track density for induced fission tracks; ρ_d is the track density for the CN5 glass standard; and ξ is the Zeta constant, which is 391 ± 17.8 in this study.

Vitrinite reflectance can provide an accurate temperature range for fission track annealing and evidence for thermal history modelling (Sweeney and Burnham, 1990; George et al., 2001). The equivalent vitrinite reflectance calculated by bitumen reflection (Feng and Chen, 1988) in the Lower Camburian Niutitang shale is in the range of 1.86–2.54% (Tian et al., 2019), and the range of 2.98–3.03% in the Lower Cambrian Jianzhuba mudstone which is adjacent to the Lower-Middle Ordovician in NDBS (**Table 1**), reflecting exmaximum paleotemperatures of 233.4°C–273.3°C and 294°C–295 °C according to Barker and Pawlewicz (1986). These results demonstrate that fission tracks in apatite were completely annealed in a geological episode and that the apatite fission tracks were all new tracks through the partial annealing zone (PAZ).

The apparent age of the AFT has no direct geological relevance (Gleadow et al., 2002). However, the thermal history simulation combined with the length distribution of the fission track and the annealing kinetic parameters of apatite itself can well reveal the thermal history experienced by the sample. To achieve robust thermal histories, inverse modelling of AFT data was carried out using the programme HeFTy (version 1.8.3, Ketcham, 2014). Model paths between specified time–temperature constraints were chosen to be monotonic rather than monotonically consistent in HeFTy. This choice provides more freedom in model paths between constraint points. Dpar was used as a kinetic parameter, and thermal histories were calculated using a multikinetic annealing model. The Kolmogorov-Smirnov test function was used to compare measured length histograms to model results (Ketcham et al., 2007). The initial mean track length was calculated based on Dpar (Carlson et al., 1999). The number of fitting curves was set to 20,000. The model quality was judged by the goodness of fit (GOF). Generally, a GOF value greater than 0.05 indicates acceptable simulation results, while a GOF value greater than 0.5 indicates high-quality simulation results (Ketcham, 2005).

RESULTS AND DISCUSSION

Apatite Fission Track Ages and Lengths

The fission track test results of all samples are shown in **Table 2**. The AFT ages of the sandstone and siltstone range from 34 Ma to 50 Ma, which are much younger than the ages of the corresponding sedimentary formations. These results indicate that the samples were all affected by thermal events and annealed after formation. Except for the F-B-4 sample, the other eight samples all pass the age χ^2-test (P (χ^2)>5%),

TABLE 1 | The homogenization temperature and equivalent vitrinite reflectance of samples.

Sample number	Sample location/adjacent strata	Equivalent vitrinite reflectance (*VRo*/%)	Paleogeotemperature (*Tmax*/°C)	Homogenization temperature (*Th*/°C)
C-2	$\epsilon_1 n$	2.0	242	181.4–194.7
F-B-3	$\epsilon_1 c/\epsilon_1 n$	—	—	368.4–398.7
B-14	$\epsilon_1 n$	2.0	242	189.0–196.7
P-1	$O_1 d/\epsilon_1 j$	< 2.98–3.03	< 294–295	—
L-1	$O_{1\text{-}2} q/\epsilon_1 j$	< 2.98–3.03	< 294–295	278.4–311.6
Z-7	$O_{1\text{-}2} q/\epsilon_1 j$	< 2.98–3.03	< 294–295	248.6–308.7
Z-8	$O_{1\text{-}2} q/\epsilon_1 j$	< 2.98–3.03	< 294–295	271.2–308.7
Z-20	$O_{1\text{-}2} q/\epsilon_1 j$	< 2.98–3.03	< 294–295	—

TABLE 2 | Results of AFT analysis in the Micangshan and Dabashan areas.

Sample number	Elevation/ m	Era	N	ρ_s (10^5/ cm^2)	Ns	ρ_i (10^5/ cm^2)	Ni	ρ_d (10^5/ cm^2)	Nd	P (χ^2) (%)	Pool AFT ages (±1σ) (Ma)	Central AFT age (±1σ) (Ma)	Mean AFT length (μm) (n)	Mean Dpar (Ranger) (μm)
B-14	817.0	$\epsilon_1 n$	35	4.237	516	12.628	1,538	7.428	5,949	82.7	49 ± 3	49 ± 3	13.0 ± 1.6 (110)	1.45 (1.15–1.63)
C-2	1,442.0	$\epsilon_1 n$	35	3.622	277	9.401	719	5.803	5,949	99.3	44 ± 4	44 ± 4	13.2 ± 1.8 (100)	1.62 (1.1–2.1)
F-B-3	1,104.0	$\epsilon_1 c$	35	3.248	508	9.623	1,505	6.13	5,949	8.4	40 ± 3	41 ± 3	12.8 ± 1.8 (101)	1.79 (1.3–2.6)
F-B-4	1,033.0	$\epsilon_1 x$	35	6.105	1,091	15.646	2,796	6.453	5,949	0.7	49 ± 3	49 ± 4	11.7 ± 2.4 (101)	1.67 (1.2–2.3)
Z-7	391.0	$O_1 d$	35	0.856	201	2.64	620	7.103	5,949	100.0	45 ± 4	45 ± 4	12.7 ± 2.3 (64)	1.41 (1.0–2.7)
Z-8	404.0	$O_{1\text{-}2} q$	35	1.748	228	5.044	228	7.428	5,949	65.4	50 ± 5	50 ± 5	12.4 ± 2.2 (51)	1.52 (1.1–2.8)
Z-20	402.0	$O_{1\text{-}2} q$	30	0.983	133	3.149	426	5.722	5,949	76.5	34 ± 4	34 ± 4	12.2 ± 2.3 (10)	1.55 (0.96–2.4)
P-1	489.0	$O_1 d$	35	1.539	128	3.559	296	5.884	5,949	94.9	50 ± 6	50 ± 6	12.0 ± 2.3 (22)	1.68 (1.0–3.2)
L-1	658.2	$O_{1\text{-}2} q$	35	0.679	113	1.864	310	6.13	5,949	100.0	44 ± 5	44 ± 5	12.5 ± 2.5 (38)	1.43 (0.9–2.4)

indicating that the age difference of a single particle is within the statistical error range and is the same age component. The pooled age is generally used as the AFT age. The sample age χ^2-test of F-B-4 is less than 5%, representing the mixed age of different provenance minerals, and the central age can be used to interpret the cooling event (Galbraith and Laslett, 1993; Sobel et al., 2006). The samples collected from the Micangshan area have a short north-south axial distance, and the AFT ages mainly range from 40 Ma to 49 Ma. The ages of the Z-7, Z-8, P-1, and L-1 samples in the northeastern part of the Dabashan belt range from 44 Ma to 50 Ma, which is considerably older than that of sample Z-20 in the southwest with an AFT age of 34 Ma. This difference may indicate that the Dabashan thrust nappe belt was uplifted from NE to SW.

The average measured AFT lengths of the samples are in the range of 11.7–13.2apatite fission trackμm, all of which are less than the original track lengths (generally exceeding 16 μm, Gleadow, 1986; Carlson et al., 1999), indicating that the samples underwent strong annealing. The distribution pattern of track lengths is generally unimodal (**Figure 3A**), and the peak values are mainly distributed in the range of 13–15 μm, indicating that the samples did not experience a multistage thermal history but were in the process of monotonic cooling (Gleadow, 1986), which may reflect rapid stripping and cooling during the later orogeny.

N, induced number of apatite grains; ρ_s, ρ_i and ρ_d, track densities for spontaneous fission tracks, induced fission tracks and CN5 glass standard tracks, respectively; Ns, Ni and Nd, number of spontaneous fission tracks counted, induced fission tracks counted and CN5 glass standards, respectively; P (χ^2), chi-square probability; L, mean track length; n, number of tracks measured.

Collectively, Dpar is a good potential indicator of fission track annealing kinetic properties in natural apatite grains (Carlson et al., 1999). The Dpar content is a routinely used parameter, exhibits a strong and informative correlation with apatite fission-track ages and lengths (**Figure 3B**). It should be noted that the lithological heterogeneity and chemical composition of samples might be different, for example the Dpar with diameters of 1.8–5.0 μm (Richardson et al., 2008), resulting in uncertainty and a negative impact on the basin-scale exhumation and

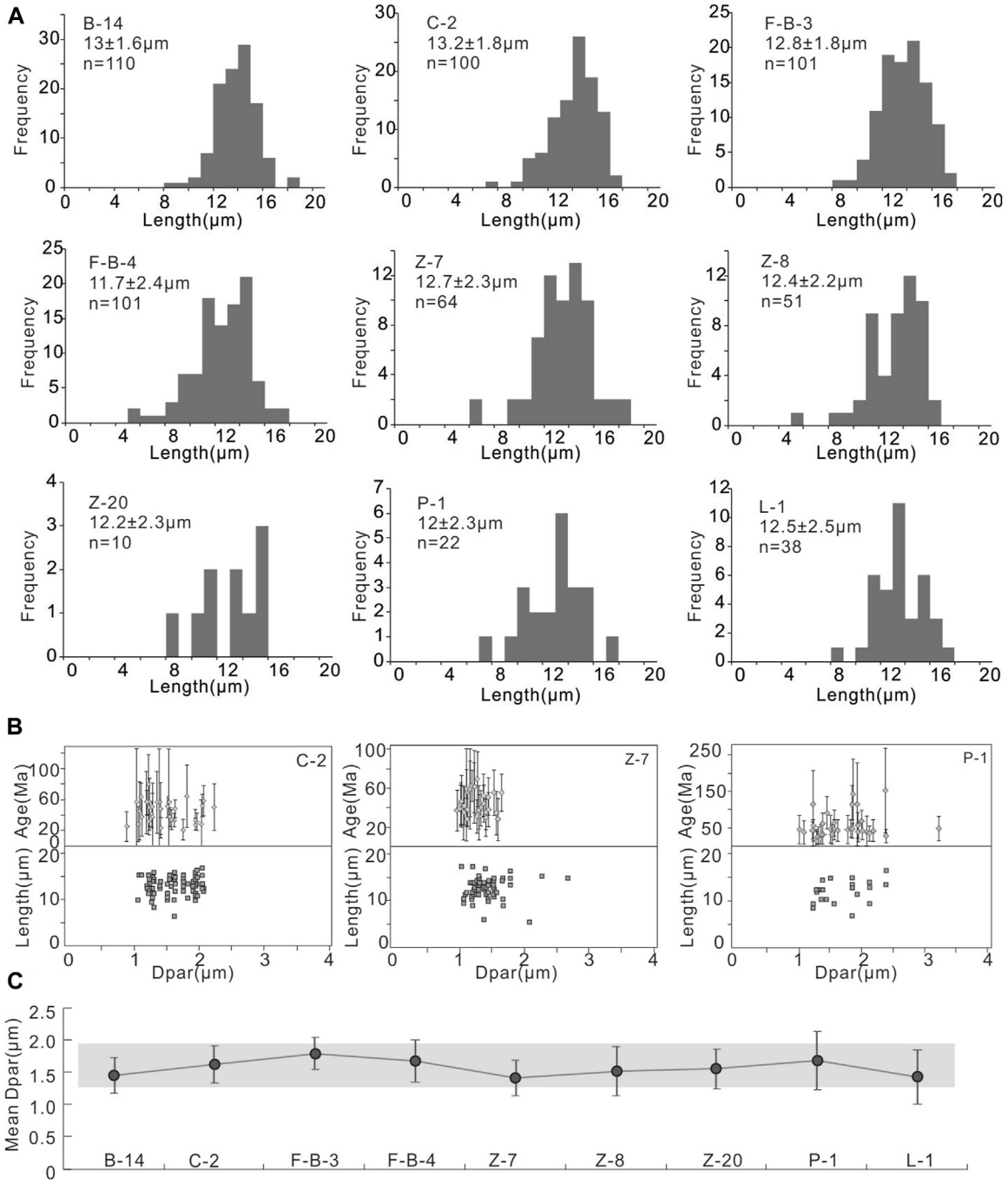

FIGURE 3 | (A) Histogram of the measured track length distribution of all samples, **(B)** relationship between Dpar and length and ages, taking samples C-2, Z-7, and P-1 for example, **(C)** Dpar plots of samples.

tectono-thermal processes. In this study, the Dpar values (mean etch pit size parallel to the c axis, Donelick, 1993) of the samples range from 1.41 to 1.79 μm (**Figure 3C**). No significant Dpar variation was observed among the samples reported in this work, in which the single-grain ages and length came from the same kinetic population. The Dpar results suggest that the differences in AFT age and length are due to the differences in thermal history and may not influenced by nature of apatite itself.

There is a positive correlation between the fission track age and the elevation of the samples, which reflects that the samples in high-altitude localities always passed through the annealing zone of apatite and produced tracks (Shen et al., 2007). However, the study area at the junction of the Qinling orogenic belt and

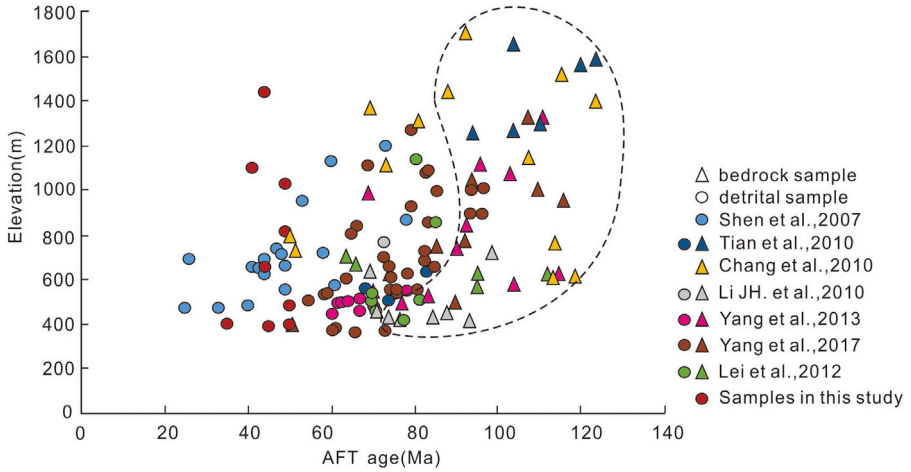

FIGURE 4 | Correlation between AFT ages and elevation.

Sichuan Basin, coupled with continuing subduction collision since the Indo-Chinese epoch and intracontinental orogeny, caused the large-scale thrust nappe (Wang et al., 2004; Shen et al., 2007; Chang et al., 2010). The elevation and distribution of apatite often change due to thrust nappes, uplift, denudation and faulting. Therefore, there is often no correlation between the fission track age and elevation in complex tectonic belts (Green et al., 1986; Shen et al., 2007; Qi et al., 2016).

Statistical analysis of fission track ages and elevations in the study area and its surrounding structural belt indicates that it underwent complex tectonic processes (**Figure 4**). The fission track ages of some sections have a good corresponding relation with altitude, but the slopes are quite different, which shows that the tectonic uplift effect is obviously different in the area. The different uplift effects may be related to the peripheral structural belt of acute Himalayan activity, especially with the far-field effect of the rapid expansion of regional topography and strong reformation from the northeastern margin of the Qinghai-Tibet Plateau (Tian et al., 2010; Tian et al., 2012; Yang et al., 2013, Yang et al., 2017). In this study, there was no linear correlation between AFT age and elevation. In addition to the complex geological process, this lack of correlation may also be related to the concentrated distribution of the topographic elevation of the samples in the smaller ranges of 391–658.2 m and 817–1442.2 m, which are insufficient to reflect the linear relationship between AFT ages and elevation.

In terms of the relationship between sample lithology and age, the ages of the samples from the outcropping area of the bedrock are generally higher than those of the detrital rocks in the sedimentary area (**Figure 4**). The AFT ages of the detrital rocks are mainly distributed in the range of 28.3–85 Ma, and those of the bedrock are mainly distributed in the range of 71–123.5 Ma. As old rigid blocks with weak detachment, the bedrock outburst area in the study area and its surrounding area responds more quickly to tectonic activities such as thrust nappes or intracontinental orogenies that cause formation uplift, and the apatite distributed in the area enters the PAZ earlier and resets its age. Micangshan-Dabashan was a passive continental margin in the early Paleozoic, and the samples from the formation were typical marine sediments. The Micangshan massif formed in the Late Triassic (Tian et al., 2010), and the provenance of the samples was not from this massif. Even if there are other provenance inputs, thermal relocation occurs with increasing burial depth and temperature after the detrital particles are transported and deposited. Therefore, the clastic apatite fission tracks reflect the late tectonic and thermal evolution of the sedimentary area rather than the provenance area. The simulation of the thermal evolutionary history of wells HY-1 and SND-1 in the study area indicates that the maximum paleo-geotemperature exceeded 220°C at 160 Ma. The Cambrian-Ordovician system at 123.5–71 Ma was buried at a depth of more than 4,000 m and had high paleo-geotemperatures ranging from 120°C to 190°C (Tian et al., 2020), and apatite did not enter the annealing zone. Then, the apatite from the Cambrian-Ordovician system entered the annealing zone with subsequent rapid uplift, so the uplift and cooling events recorded by the fission track ages were relatively late. Overall, the Micangshan-Dabashan tectonic belt experienced uplift and denudation from at least 123.5 Ma and affected the surrounding sedimentary strata, entering the PAZ from 85 Ma to 28.3 Ma.

The AFT age and length are positively correlated to a certain extent according to the data in the research area (**Figure 5**). The AFT ages gradually become younger from the Micangshan-Hannan massif to the northern Sichuan Basin, indicating a gradual thrust expansion from north to south in the region as piggyback expansion (Tian et al., 2010; Yang et al., 2013; Wang et al., 2003). In this tectonic framework, the AFT ages of the Cambrian strata samples in the Huijunba syncline should be larger than those in the northern Sichuan foreland area. However, the AFT ages of the Cretaceous-Cambrian stratum samples in the northern Sichuan foreland area range from 61.6 to 85 Ma with the track lengths between 10.6 and 12.2 μm and that in Huijunba syncline at the range of 40–49 Ma with track lengths between 11.7 and 13.2 μm (**Figure 5A**). This distribution of AFT ages and

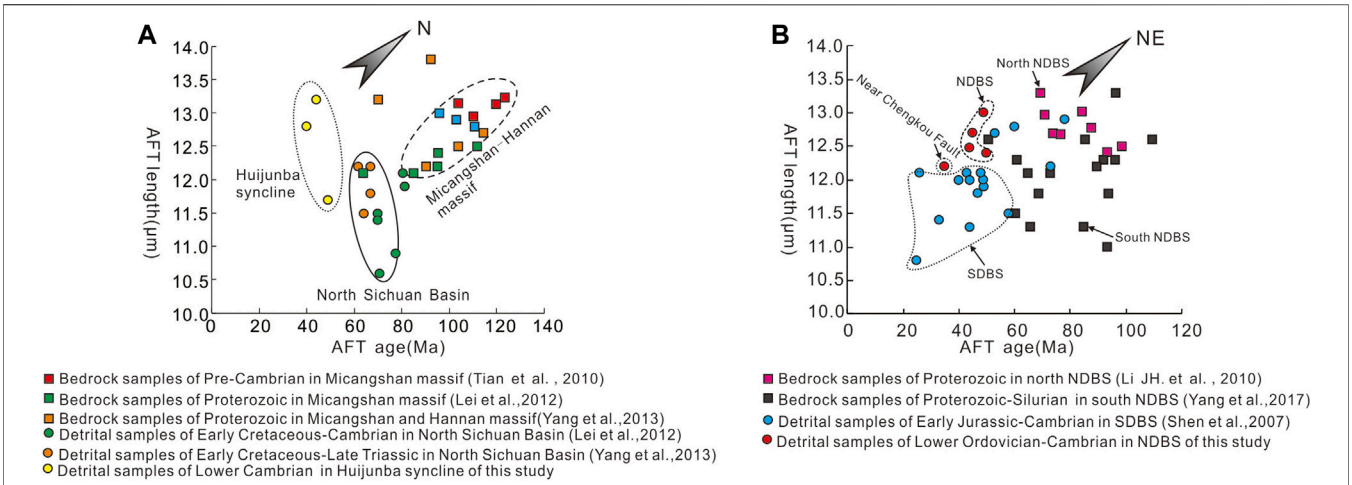

FIGURE 5 | Correlation between AFT ages and lengths of the measured rock samples in the Micangshan area **(A)** and Dabashan area **(B)**.

lengths seems inconsistent with regional tectonic evolution history. Micangshan tectonic zone is a large complex anticline formed by South Qinling collision orogeny since the Triassic and is characterized by the asymmetric structure with a gentle north wing orienting Huijunba syncline and steep south wing orienting north Sichuan foreland (Zhang and Dong, 2009; Zhang, 2019). The samples in the Sichuan foreland area was deeper than samples in the north Huijunba syncline. Therefore, these abnormal AFT ages may be caused by differential basement uplift, as the sedimentary cover in the northern Sichuan foreland area uplifted and entered the PAZ earlier than that in the Huijunba syncline during the overall N-S trending uplift process.

Generally, the AFT age from Dabashan area gradually becomes younger from NE to SW, indicating that the timing of uplift in the NE region was earlier than that in the SW (Shen et al., 2007; Li JH. et al., 2010; Yang et al., 2017, **Figure 5B**). In this study, the AFT age of the NDBS ranges from 35 Ma to 50 Ma, the youngest age of NDBS sample Z-20 is located near the Chengkou fault. Collectively, the AFT ages from the NDBS are older than most ages from the SDBS (**Figure 5B**). This distribution of AFT ages indicates that the uplift process of the sedimentary cap is characterized by earlier to NE and later to SW under the influence of regional uplift. This interpretation is consistent with the thrust nappe of Dabashan from NE to SW (Shen et al., 2007) and the NE-SW trending paleo-tectonic stress during the Late Jurassic to the Early Cretaceous (Shi et al., 2012; Dong et al., 2014). The analysis of AFT provides a new thermochronological constraint for the progressive extension deformation of the thrust nappe structure in the Dabashan area.

Tectono-Thermal History of the Micangshan-Dabashan Tectonic Belt

Geological background constraints are very important for the inversion of the AFT thermal history (Tian et al., 2010). In the study area, many major geological events occurred during the Jurassic and Cretaceous, and the Qinling orogenic belt truly entered the intracontinental orogenic deformation period at approximately 160 Ma (Dong et al., 2006). The Micangshan-Dabashan tectonic belt, as the southern margin of the Qinling orogenic belt, likely responded to this tectonic event. Previous AFT data and thermal simulation results showing that Dabashan area experienced uplift at 180–165 Ma, 170–160 Ma and ca.100 Ma (Shen et al., 2007; Li JH et al., 2010; Xu et al., 2010), and the Micangshan area experienced uplift at 140–100 Ma and 152–150 Ma (Tian et al., 2010; Tian et al., 2012; Xu et al., 2010), which have also provided important constraints for the thermal simulation.

To constrain the maximum paleo-geotemperature experienced by the samples, paleotemperature scales such as vitrinite reflectance are always used along with homogenization temperatures of fluid inclusions in or adjacent to the strata where the samples were located (**Table 1**). In the Micangshan area, the inclusion samples collected from the Lower Cambrian Niutitang Formation were emplaced at 212–166 Ma (Tian et al., 2020). The organic fluids in the Dabashan areas were captured in the Late Triassic to Early-Middle Jurassic (Li RX. et al., 2012). Therefore, the vitrinite reflectance and homogenization temperature of organic fluids were used in this study to constrain the maximum paleogeotemperature in the Late Triassic to Early-Middle Jurassic. The F-B-3 and F-B-4 samples are not representative because of the effect of regional thermal anomalies (Tian et al., 2020), and the AFT age χ^2-test is less than 5%, which reflects the thermal history of different provenances. Thermal history inversion simulations were carried out for samples other than F-B-3 and F-B-4 under the geological constraints in this paper.

The inversely modelled t-T paths for the samples collected from the Micangshan-Dabashan tectonic zone are shown in **Figure 6**. The simulated age and track length GOF values of all samples are greater than 0.5 and indicate that high-quality thermal simulation results are obtained. The sedimentary areas of Micangshan and Dabashan have experienced similar cooling histories since the Late Jurassic (160 Ma), presenting a continuous and single uplift and cooling process. This relatively rapid cooling at ca.160 Ma is consistent with that in Micangshan-Hannan massif at 150 Ma

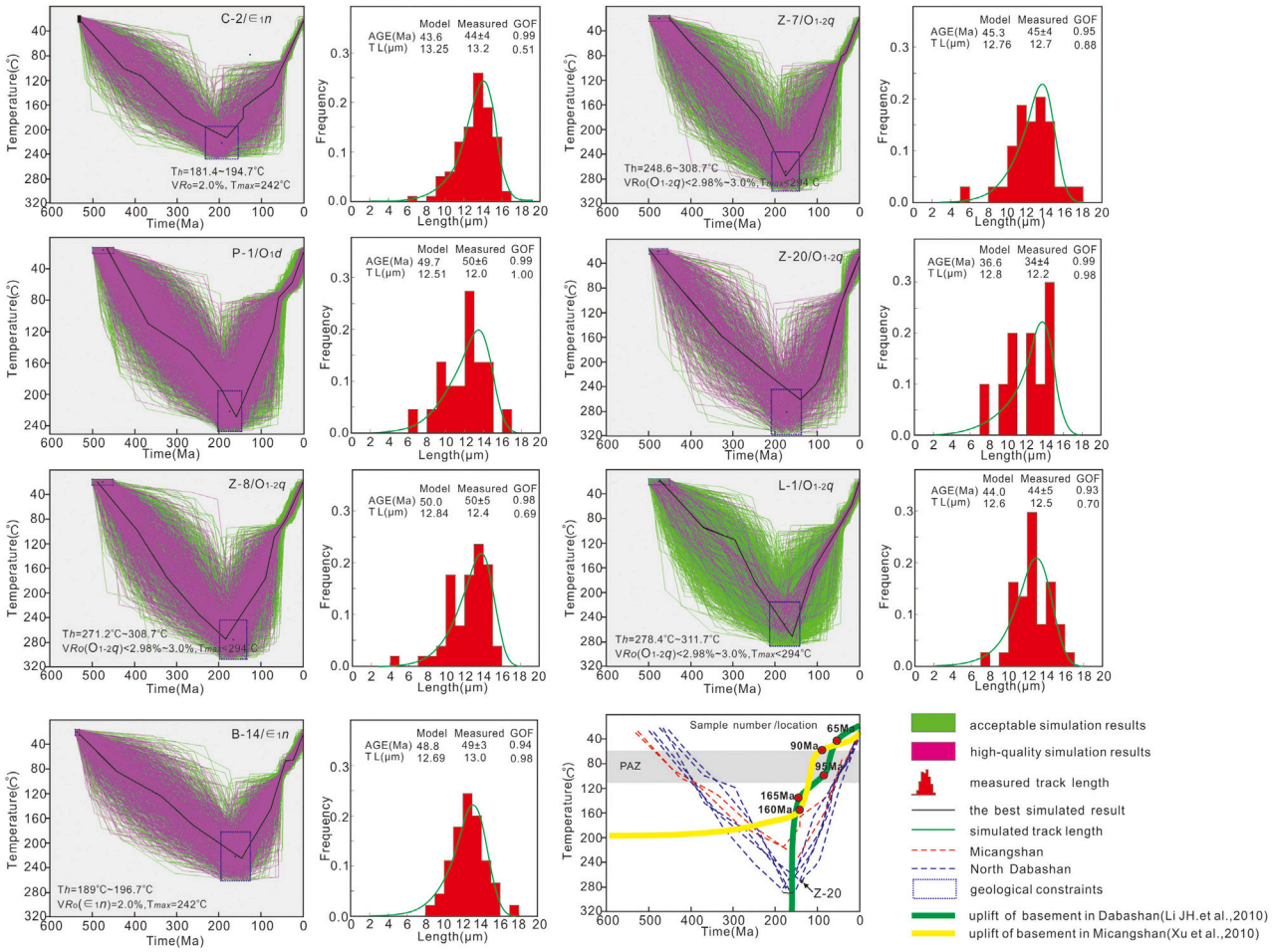

FIGURE 6 | Results of thermal history modelling based on apatite fission track (AFT) data using HeFTy for samples from the Micangshan and Dabashan tectonic belts. The rapid cooling time of sample Z-20 near the Chengkou fault was later than the others, which may indicate the cooling event in the Dabashan area was gradual from northeast to southwest (NS-SW).

and Dabashan tectonic zone at 153 Ma (Xu et al., 2010), which is a precise response to the event of Qinling orogenic belt entered the intracontinental orogenic deformation period (Dong et al., 2006; Li et al., 2013). However, this cooling time is much earlier than that in the southwestern Qinling (Late Cretaceous, Enkelmann et al., 2006), east Qinling-Dabieshan (ca.100 Ma, Hu et al., 2006) and Longmenshan tectonic zone (119–131 Ma, Arne et al., 1997). The previous work shows that it is possibly a response to the combined effects of the Mesozoic tectonism in nearby regions, which probably reactivated pre-existing structures through strike-slip faulting (Webb et al., 1999; Hu et al., 2006; Tian et al., 2012). The Yangtze Block rotated clockwise relative to the north China block through Mesozoic time (Sun et al., 2006) may be an important inducement. The Micangshan-Dabashan area is the core area of the deformation of rotated clockwise that uplift and cooling earlier due to the dextral extrusion. And then spread to the further and more marginal areas such as southwestern Qinling, eastern Qinling-Dabie and Longmenshan tectonic zone. Furthermore, the rapid cooling of Micangshan-Dabashan area at ca.160 Ma was probably the northern source for the early Cretaceous deposition in the northern Sichuan Basin (Meng et al., 2005; Tian et al., 2012). On the background of uplift in the region, the basement and sedimentary cap in Micangshan-Dabashan area also underwent different uplifting processes.

The Micangshan area was uplifted as a whole during 160–90 Ma, and the sedimentary strata and basement experienced a relatively consistent regional uplift process. The sedimentary strata uplifted differently from the basement since 90 Ma. Under the action of thrust and nappe tectonics, the rigid basement uplifted slowly and horizontally, and the plastic strata were squeezed and deformed, which produced the characteristics of folding and uplift since 90 Ma and then entered the PAZ at 63 Ma. Previous study concluded that the displacement of upper structure in Micangshan area is larger than the lower during the progressive deformation process of contraction orogenesis from north to south based on the analysis of structural types and geometric evolution characteristics of folds (Ramsay and Lisle, 2000; Zhang, 2019). And our finding of the different uplifting processes of basement and sedimentary cap is comparable with previous results.

In the Dabashan area, the uplift of sedimentary strata was different from that of the basement during 165–95 Ma. The basement uplifted relatively slowly, while the sedimentary strata uplifted rapidly due to strong fold deformation. The sedimentary strata and the basement experienced a relatively consistent regional uplift process from 95 Ma to 65 Ma. After 65 Ma, the strata experienced differential uplift again (**Figure 6**). In the process of Dabashan nappe extrusion, the rapid uplift of the lower Paleozoic strata in the NDBS since 160 Ma occurred much earlier than that of the Paleozoic strata in the SDBS since ca. 100 Ma (Shen et al., 2007), which reflects the process of nappe uplift from north to south in the Dabashan area. The occurrence of differential uplift between sedimentary strata and basement may reflect the different intensities of thrust and nappe in different stages.

Abundant AFT ages of Late Cenozoic have been used to explain the rapid northeastward growth of Tibetan Plateau, such as ca.20 Ma in northern Longmenshan, 13–15 Ma in central and south Longmenshan and ca.13 Ma in the eastern Tibetan Plateau. Most of the samples which revealed the accelerated cooling were exposed basement samples and shallow buried Cretaceous-Permian samples. However, the simulation results in this study do not show the obvious accelerated cooling in the Late Cenozoic. The accelerated cooling of northeastern Tibet Plateau since Late Cenozoic was the result of multiple factors, which was not only the eastward growth of the Tibetan Plateau, but also intensified by climate change in Southeast Asia (Molnar and Tapponnier, 1975; Tian et al., 2012) and the erodibility of the drainage systems that accelerated the denudation (Richardson et al., 2008; Richardson et al., 2010). Our new samples were from the deep Cambrian-Ordovician strata and they are still buried deeply lager than 2 km (Tian et al., 2020) and was less affected by climate and water erosion in the Late Cenozoic. These may be the reasons why the cooling process was not significantly accelerated in this thermal simulation since the Late Cenozoic.

CONCLUSION

The detrital AFT thermochronological dataset provide new insight into the Meso-Cenozoic tectono-thermal evolution of the Micangshan-Dabashan tectonic belt, central China. New evidence leads us to draw the following conclusions:

1) The AFT ages and lengths suggest that the cooling events in the Micangshan area were gradual from north to south and different uplift occurred on both sides of Micangshan massif. The cooling in Dabashan tectonic zone was from northeast to southwest.
2) A relatively rapid cooling since ca.160 Ma occurred in the Micangshan-Dabashan area which was a precise response to the event of Qinling orogenic belt entered the intracontinental orogenic deformation period. The cooling event may relate to the northeastward dextral compression of the Yangtze Block.
3) The cooling processes of basement and sedimentary cap in Micangshan-Dabashan tectonic belt were inconsistent under the thrust and nappe action. The rigid basement was not always continuous and rapidly uplifted or mainly showed as lateral migration in a certain stage and the plastic sedimentary strata rapidly uplifted due to intense folding deformation and entered the PAZ since ca. 63 Ma.
4) The deep buried samples in Micangshan-Dabashan tectonic belt may be less affected by climate and water erosion what intensified the cooling so that the accelerated cooling was not obvious in the Late Cenozoic as usual.

DATA AVAILABILITY STATEMENT

The original contributions presented in the study are included in the article/Supplementary Material, further inquiries can be directed to the corresponding author.

AUTHOR CONTRIBUTIONS

TT: Conceptualization, Methodology, Resources, Data Curation, Writing-Original Draft, Review and Editing and Project administration. PY: Conceptualization, Methodology, Validation, Formal analysis, Data Curation, Writing-Original Draft, Review and Editing and Visualization. JY: Methodology, Supervision, Project administration and Funding acquisition. ZD: Methodology, Supervision, Writing-Review and Editing, Project administration and Funding acquisition. ZR: Conceptualization, Methodology, Writing-Review and Editing. DF: Formal analysis and Investigation. FY: Formal analysis and Investigation.

FUNDING

This study was supported by the Key Project of Shaanxi Coal Geology Group Co., Ltd., (Grant No. SMDZ (KY)-2020-004), the Independent Project of the Key Laboratory of Coal Exploration and Comprehensive Utilization, MNR (Grant No. ZP 2019-2), and the National Natural Science Foundation of China (Grant No. 41630312, 42102164).

ACKNOWLEDGMENTS

We are grateful to science editor Xuhua Shi for handing with our manuscript. The editors and two reviewers are thanked for critical and constructive comments.

REFERENCES

Arne, D., Worley, B., Wilson, C., Chen, S. F., Foster, D., Luo, Z. L., et al. (1997). Differential Exhumation in Response to Episodic Thrusting along the Eastern Margin of the Tibetan Plateau. *Tectonophysics* 280, 239–256. doi:10.1016/s0040-1951(97)00040-1

Barker, C. E., and Pawlewicz, M. J. (1986). "The Correlation of Vitrinite Reflectance with Maximum Temperature in Humic Organic Matter," in *Paleogeothermics, Heidellberg*. Editors G. Buntebarth and L. Stegena (Berlin: Springer), 79–93.

Bellemans, F., De̋Corte, F., and Van Den̈Haute, P. (1995). Composition of SRM and CN U-Doped Glasses: Significance for Their Use as thermal Neutron Fluence Monitors in Fission Track Dating. *Radiat. Measurements* 24, 153–160. doi:10.1016/1350-4487(94)00100-f

Carlson, W. D., Donelick, R. A., and Ketcham, R. A. (1999). Variability of Apatite Fission-Track Annealing Kinetics; I, Experimental Results. *Am. Mineral.* 84, 1213–1223. doi:10.2138/am-1999-0901

Chang, Y., Xu, C. H., Peter, W. R., and Zhou, Z. Y. (2010). The Exhumation Evolution of the Micangshan-Hannan Uplift since Cretaceous Evidences from apatite(U-Th)/He Dating. *Chin. J. Geophys.* (in Chinese) 53, 912–919. doi:10.3969/j.issn.000125733.2010.04.016

Cheng, R. H., Wang, P. J., Liu, W. Z., Tang, H., Bai, Y., Kong, Q., et al. (2004). Response of Triassic Sequence Stratigraphy of Lower Yangtze to Collision between Yangtze Plate and North China Plate. *Geotectonica et Metallogenia* 29 (2), 174–184.

Clark, M. K., Schoenbohm, L. M., Royden, L. H., Whipple, K. X., Burchfiel, B. C., Zhang, X., et al. (2004). Surface Uplift, Tectonics, and Erosion of Eastern Tibet from Large-Scale Drainage Patterns. *Tectonics* 23, TC1006. doi:10.1029/2002TC001402

Dong, S. W., Hu, J. M., Shi, W., Zhang, Z. Y., and Liu, G. (2006). Jurassic Superposed Folding and Jurassic Foreland in the Daba Mountain, Central China. *Acta Geoscientia Sinica*. (in Chinese) 27, 403–410. doi:10.3321/j.issn:1006-3021.2006.05.003

Dong, S. W., Zhang, Y. Q., Li, Q. S., Gao, R., Hu, J. M., Shi, W., et al. (2014). *Study on the Daba Mountain Intra-continental Orogen belt*. Beijing: Geological Publishing House, 83–108. (in Chinese).

Dong, Y. P., Zha, X. F., Fu, M. Q., Zhang, Q., Yang, Z., and Zhang, Y. (2008). Characteristics of the Dabashan Fold-Thrust Nappe Structure at the Southern Margin of the Qinling, China. *Geol. Bull. China*. (in Chinese) 27, 1493–1508.

Du, D. D., Zhang, C. J., Mughal, M. S., Wang, X. Y., Blaise, D., Gao, J. P., et al. (2018). Detrital Apatite Fission Track Constraints on Cenozoic Tectonic Evolution of the Northeastern Qinghai-Tibet Plateau, China: Evidence from Cenozoic Strata in Lulehe Section, Northern Qaidam Basin. *J. Mt. Sci.* 15, 532–547. doi:10.1007/s11629-017-4692-5

Enkelmann, E., Ratschbacher, L., Jonckheere, R., Nestler, R., Fleischer, M., Gloaguen, R., et al. (2006). Cenozoic Exhumation and Deformation of Northeastern Tibet and the Qinling: Is Tibetan Lower Crustal Flow Diverging Around the Sichuan Basin. *Geol. Soc. America Bull.* 118, 651–671. doi:10.1130/b25805.1

Feng, G. X., and Chen, S. J. (1988). Relationship between the Reflectance of Bitumen and Vitrinite in Rock. *Nat. Gas Industry*. (in Chinese) 3, 30–35.

Galbraith, R. F., and Laslett, G. M. (1993). Statistical Models for Mixed Fission Track Ages. *Nucl. Tracks Radiat. Measurements* 21, 459–470. doi:10.1016/1359-0189(93)90185-c

Gallagher, K. (2003). Fission Track Analysis and its Applications to Geological Problems. *Annu. Rev. Earth Planet. Sci.* 26, 519–572. doi:10.1146/annurev.earth.26.1.519

George, A. D., Marshallsea, S. J., Wyrwoll, K.-H., Jie, C., and Yanchou, L. (2001). Miocene Cooling in the Northern Qilian Shan, Northeastern Margin of the Tibetan Plateau, Revealed by Apatite Fission-Track and Vitrinite-Reflectance Analysis. *Geol* 29, 939. doi:10.1130/0091-7613(2001)0292.0.co;2

Gleadow, A. J. W., Belton, D. X., Kohn, B. P., and Brown, R. W. (2002). Fission Track Dating of Phosphate Minerals and the Thermochronology of Apatite. *Rev. Mineralogy Geochem.* 48, 579–630. doi:10.2138/rmg.2002.48.16

Gleadow, A. J. W., Duddy, I. R., Green, P. F., and Lovering, J. F. (1986). Confined Fission Track Lengths in Apatite: a Diagnostic Tool for thermal History Analysis. *Contr. Mineral. Petrol.* 94, 405–415. doi:10.1007/bf00376334

Godard, V., Pik, R., Lave, J., Cattin, R., Tibari, B., sigoyer, J. D., et al. (2009). Late Cenozoic Evolution of the central Longmen Shan, Eastern Tibet: Insight from (U-Th)/He Thermochronometry. *Tectonics* 28, TC5009. doi:10.1029/2008tc002407

Green, P. F., Duddy, I. R., Gleadow, A. J. W., Tingate, P. R., and Laslett, G. M. (1986). Thermal Annealing of Fission Tracks in Apatite. *Chem. Geology. Isotope Geosci. section* 59, 237–253. doi:10.1016/0168-9622(86)90074-6

Green, P. F. (1988). The Relationship between Track Shortening and Fission Track Age Reduction in Apatite: Combined Influences of Inherent Instability, Annealing Anisotropy, Length Bias and System Calibration. *Earth Planet. Sci. Lett.* 89, 335–352. doi:10.1016/0012-821x(88)90121-5

He, J. K., Lu, H. F., Zhang, Q. L., and Zhu, B. (1997). The Trust Tectonics and Transpressive Geodynamics in Southern Dabashan Mountains. *Geol. J. China Universities*. (in Chinese) 3, 419–428.

Homke, S., Vergés, J., Van Der Beek, P., Fernàndez, M., Saura, E., Barbero, L., et al. (2010). Insights in the Exhumation History of the NW Zagros from Bedrock and Detrital Apatite Fission-Track Analysis: Evidence for a Long-Lived Orogeny. *Basin Res.* 22, 659–680. doi:10.1111/j.1365-2117.2009.00431.x

Hu, S., Kohn, B. P., Raza, A., Wang, J., and Gleadow, A. J. W. (2006). Cretaceous and Cenozoic Cooling History across the Ultrahigh Pressure Tongbai-Dabie belt, central China, from Apatite Fission-Track Thermochronology. *Tectonophysics* 420, 409–429. doi:10.1016/j.tecto.2006.03.027

Huang, W., and Wu, Z. W. (1992). Evolution of the Qinling Orogenic Belt. *Tectonics* 11, 371–380. doi:10.1029/91tc02419

Hurford, A. J., and Green, P. F. (1983). The Zeta Age Calibration of Fission-Track Dating. *Chem. Geology.* 41, 285–317. doi:10.1016/s0009-2541(83)80026-6

Hurford, A. J. (1990). Standardization of Fission Track Dating Calibration: Recommendation by the Fission Track Working Group of the I.U.G.S. Subcommission on Geochronology. *Chem. Geology. Isotope Geosci. section* 80, 171–178. doi:10.1016/0168-9622(90)90025-8

Ketcham, R. A., Carter, A., Donelick, R. A., Barbarand, J., and Hurford, A. J. (2007). Improved Measurement of Fission-Track Annealing in Apatite Using C-axis Projection. *Am. Mineral.* 92, 789–798. doi:10.2138/am.2007.2280

Ketcham, R. A. (2005). Forward and Inverse Modeling of Low-Temperature Thermochronometry Data. *Rev. Mineralogy Geochem.* 58, 275–314. doi:10.2138/rmg.2005.58.11

Ketcham, R. A. (2014). *HeFTy Version 1.8.3*. Austin: University of Texas.

Kirby, E., Reiners, P. W., Krol, M. A., Whipple, K. X., Hodges, K. V., Farley, K. A., et al. (2002). Late Cenozoic Evolution of the Eastern Margin of the Tibetan Plateau: Inferences from 40Ar/39Ar and (U-Th)/He Thermochronology. *Tectonics* 21, 1001. doi:10.1029/2000tc001246

Lei, Y. L., Jia, C. Z., Li, B. L., Wei, G., Chen, Z., and Shi, X. (2012). Meso-Cenozoic Tectonic Events Recorded by Apatite Fission Track in the Northern Longmen-Micang Mountains Region. *Acta Geologica Sinica* 86, 153–165. doi:10.1111/j.1755-6724.2012.00618.x

Li, J., Dong, S., Yin, A., Zhang, Y., and Shi, W. (2015). Mesozoic Tectonic Evolution of the Daba Shan Thrust Belt in the Southern Qinling Orogen, central China: Constraints from Surface Geology and Reflection Seismology. *Tectonics* 34, 1545–1575. doi:10.1002/2014tc003813

Li, J. H., Zhang, Y. Q., Dong, S. W., Shi, W., and Li, H. (2010). Apatite Fission Track Thermochronologic Constraint on Late Mesozoic Uplifting of the Fenghuangshan Basement Uplift. *Chin. J. Geology*. (in Chinese) 45, 969–986.

Li, J., Zhang, Y., Dong, S., and Shi, W. (2013). Structural and Geochronological Constraints on the Mesozoic Tectonic Evolution of the North Dabashan Zone, South Qinling, central China. *J. Asian Earth Sci.* 64, 99–114. doi:10.1016/j.jseaes.2012.12.001

Li, P. Y., Zhang, J. J., Guo, L., and Yang, X. (2011). Structural Features and Deformational Ages in the Front of the Northern Dabashan Thrust belt. *Earth Sci. Front.* 3, 41–49. doi:10.1016/j.gsf.2011.11.002

Li, R. X., Dong, S. W., Zhang, S. N., Zhu, R. J., and Xia, B. (2012). Features and Formation of Organic Fluids during Dabashan Orogenesis. *J. Nanjing Univ. (Natural Science).* (in Chinese) 48, 295–307. doi:10.13232/j.cnki.jnju.2012.03.005

Li, Y. F., Qu, G. S., Liu, S., and Zhang, H. (2008). Strucyural Characters and Mechanism in the Micangshan and Southern Dabashan Mountains Front. *Geotect Metal* 32, 285–292. doi:10.16539/j.ddgzyckx.2008.03.006

Li, Z. W., Liu, S., Chen, H., Deng, B., Hou, M., Wu, W., et al. (2012). Spatial Variation in Meso-Cenozoic Exhumation History of the Longmen Shan Thrust belt (Eastern Tibetan Plateau) and the Adjacent Western Sichuan basin: Constraints from Fission Track Thermochronology. *J. Asian Earth Sci.* 47, 185–203. doi:10.1016/j.jseaes.2011.10.016

Li, Z. W., Chen, H. D., Liu, S. G., Hou, M., and Deng, B. (2010). Differential Uplift Driven by Thrusting and its Lateral Variation along the Longmenshan belt, Western Sichuan, China: Evidence from Fission Track Thermochronology. *Chin. J. Geology*. (in Chinese) 45, 944–968.

Lin, X., Zheng, D., Sun, J., Windley, B. F., Tian, Z., Gong, Z., et al. (2015). Detrital Apatite Fission Track Evidence for Provenance Change in the Subei Basin and Implications for the Tectonic Uplift of the Danghe Nan Shan (NW China) since the Mid-miocene. *J. Asian Earth Sci.* 111, 302–311. doi:10.1016/j.jseaes.2015.07.007

Meng, Q. R., Wang, E., and Hu, J. M. (2005). Mesozoic Sedimentary Evolution of the Northwest Sichuan Basin: Implication for Continued Clockwise Rotation of the south China Block. *Geol. Soc. America Bull.* 117, 396–410. doi:10.1130/b25407.1

Meng, Q. R., and Zhang, G. W. (2000). Geologic Framework and Tectonic Evolution of the Qinling Orogen, central China. *Tectonophysics* 323, 183–196. doi:10.1016/s0040-1951(00)00106-2

Molnar, P., and Tapponnier, P. (1975). Cenozoic Tectonics of Asia: Effects of a Continental Collision: Features of Recent continental Tectonics in Asia Can Be Interpreted as Results of the India-Eurasia Collision. *Science* 189, 419–426. doi:10.1126/science.189.4201.419

Powell, J. W., Schneider, D. A., and Issler, D. R. (2017). Application of Multi-Kinetic Apatite Fission Track and (U-Th)/He Thermochronology to Source Rock thermal History: a Case Study from the Mackenzie Plain, NWT, Canada. *Basin Res.* 30, 497–512. doi:10.1111/bre.12233

Qi, B., Hu, D., Yang, X., Zhang, Y., Tan, C., Zhang, P., et al. (2016). Apatite Fission Track Evidence for the Cretaceous-Cenozoic Cooling History of the Qilian Shan (NW China) and for Stepwise Northeastward Growth of the Northeastern Tibetan Plateau since Early Eocene. *J. Asian Earth Sci.* 124, 28–41. doi:10.1016/j.jseaes.2016.04.009

Ramsay, J. G., and Lisle, R. J. (2000). "The Techniques of Modern Structural Geology," in *Applications of Continuum Mechanics in Structural Geology*, Vol. 3. London: Academic Press, 702–1061.

Reiners, P. W., Zhou, Z., Ehlers, T. A., Xu, C., Brandon, M. T., Donelick, R. A., et al. (2003). Post-orogenic Evolution of the Dabie Shan, Eastern China, from (U-Th)/He and Fission-Track Thermochronology. *Am. J. Sci.* 303, 489–518. doi:10.2475/ajs.303.6.489

Ren, Z. L., Cui, J. P., Guo, K., Tian, T., Li, H., Wang, W., et al. (2015). Fission-track Analysis of Uplift Times and Processes of the Weibei Uplift in the Ordos Basin. *Chin. Sci. Bull.* (in Chinese) 60, 1298–1309. doi:10.1360/N972014-00617

Richardson, N. J., Densmore, A. L., Seward, D., Fowler, A., Wipf, M., Ellis, M. A., et al. (2008). Extraordinary Denudation in the Sichuan basin: Insights from Low Temperature Thermochronology Adjacent to the Easternmargin of the Tibetan Plateau. *J. Geophys. Res.* 113, 1–23. doi:10.1029/2006jb004739,

Richardson, N. J., Densmore, A. L., Seward, D., Wipf, M., and Yong, L. (2010). Did Incision of the Three Gorges Begin in the Eocene. *Geology* 38, 551–554. doi:10.1130/g30527.1

Shen, C. B., Mei, L. F., Fan, Y. F., and Tang, J. G. (2005). Advances and Prospects of Apatite Fission Track Thermochronology. *Geol. Sci. Tech. Information*. (in Chinese) 24, 57–63.

Shen, C. B., Mei, L. F., Xu, Z. P., Tang, J. G., and Tian, P. (2007). Fission Track Thermochronology Evidence for Mesozoic-Cenozoic Uplifting of Daba Mountain, central China. *Acta Petrologica Sinica*. (in Chinese) 23, 2901–2910. doi:10.3969/j.issn.1000-0569.2007.11.020

Shen, X., Tian, Y., Zhang, G., Zhang, S., Carter, A., Kohn, B., et al. (2019). Late Miocene Hinterland Crustal Shortening in the Longmen Shan Thrust Belt, the Eastern Margin of the Tibetan Plateau. *J. Geophys. Res. Solid Earth* 124, 11972–11991. doi:10.1029/2019jb018358

Shi, H. C., and Shi, X. B. (2014). Exhumation Process of Middle-Upper Yangtze since Cretaceous and its Tectonic Significance: Low-Temperature Thermochronology Constraints. *Chin. J. Geophys*. (in Chinese) 57, 2608–2619. doi:10.1002/cjg2.20141

Shi, W., Zhang, Y., Dong, S., Hu, J., Wiesinger, M., Ratschbacher, L., et al. (2012). Intra-continental Dabashan Orocline, Southwestern Qinling, Central China. *J. Asian Earth Sci.* 46, 20–38. doi:10.1016/j.jseaes.2011.10.005

Sobel, E., Chen, J., and Heermance, R. (2006). Late Oligocene-Early Miocene Initiation of Shortening in the Southwestern Chinese Tian Shan: Implications for Neogene Shortening Rate Variations. *Earth Planet. Sci. Lett.* 247, 70–81. doi:10.1016/j.epsl.2006.03.048

Sun, Z., Yang, Z., Yang, T., Pei, J., and Yu, Q. (2006). New Late Cretaceous and Paleogene Paleomagnetic Results from south China and Their Geodynamic Implications. *J. Geophys. Res.* 111, B03101. doi:10.1029/2004JB003455

Sweeney, J. J., and Burnham, A. K. (1990). Evaluation of a Simple Model of Vitrinite Reflectance Based on Chemical Kinetics. *AAPG Bull.* 74, 1559–1570. doi:10.1306/0c9b251f-1710-11d7-8645000102c1865d

Tan, X., Kodama, K. P., Gilder, S., Courtillot, V., and Cogné, J.-P. (2007). Palaeomagnetic Evidence and Tectonic Origin of Clockwise Rotations in the Yangtze Fold belt, South China Block. *Geophys. J. Int.* 168, 48–58. doi:10.1111/j.1365-246x.2006.03195.x

Tian, T., Fu, D. L., Yang, F., Duan, Z., Lin, Y., and Zhao, X. (2018). Relationship between mineral Composition and Micro-pores of Niutitang-Formation Shale in Micangshan-Hannan Uplift. *J. China Coal Soc*. (in Chinese) 43, 236–244. doi:10.13225/j.cnki.jccs.2017.1646

Tian, T., Yang, P., Ren, Z., Fu, D., Zhou, S., Yang, F., et al. (2020). Hydrocarbon Migration and Accumulation in the Lower Cambrian to Neoproterozoic Reservoirs in the Micangshan Tectonic Zone, China: New Evidence of Fluid Inclusions. *Energ. Rep.* 6, 721–733. doi:10.1016/j.egyr.2020.03.012

Tian, T., Zhou, S., Fu, D., Yang, F., and Li, J. (2019). Calculation of the Original Abundance of Organic Matter at High-Over Maturity: A Case Study of the Lower Cambrian Niutitang Shale in the Micangshan-Hannan Uplift, SW China. *J. Pet. Sci. Eng.* 179, 645–654. doi:10.1016/j.petrol.2019.04.071

Tian, Y., Kohn, B. P., Phillips, D., Hu, S., Gleadow, A. J. W., and Carter, A. (2016). Late Cretaceous-Earliest Paleogene Deformation in the Longmen Shan Fold-And-Thrust belt, Eastern Tibetan Plateau Margin: Pre-cenozoic Thickened Crust. *Tectonics* 35, 2293–2312. doi:10.1002/2016tc004182

Tian, Y., Kohn, B. P., Zhu, C., Xu, M., Hu, S., and Gleadow, A. J. W. (2012). Post-orogenic evolution of the Mesozoic Micang Shan Foreland Basin system, central China. *Basin Research* 24, 70–90. doi:10.1111/j.1365-2117.2011.00516.x

Tian, Y. T., Kohn, B. P., Gleadow, A. J. W., and Hu, S. (2013). Constructing the Longmen Shan eastern Tibetan plateau margin: Insights from low-temperature thermochronology. *Tectonics* 32, 576–592. doi:10.1111/j.1365-2117.2011.00516.x

Tian, Y. T., Li, R., Tang, Y., Xu, X., Wang, Y., and Zhang, P. (2018). Thermochronological Constraints on the Late Cenozoic Morphotectonic Evolution of the Min Shan, the Eastern Margin of the Tibetan Plateau. *Tectonics* 37, 1–17. doi:10.1029/2017tc004868

Tian, Y. T., Zhu, C. Q., Xu, M., Rao, S., Kohn, B., and Hu, S. (2010). Exhumation History of the Micangshan-Hannan Dome since Cretaceous and its Tectonic Significance:evidences from Apatite Fission Track Analysis. *Chin. J. Geophys*. (in Chinese) 53, 920–930. doi:10.3969/j.issn.000125733.2010.04.017

Wang, E., Kirby, E., Furlong, K. P., van Soest, M., Xu, G., Shi, X., et al. (2012). Two-phase Growth of High Topography in Eastern Tibet during the Cenozoic. *Nat. Geosci* 5 (9), 640–645. doi:10.1038/ngeo1538

Wang, E., Meng, Q., Clark Burchfiel, B., and Zhang, G. (2003). Mesozoic Large-Scale Lateral Extrusion, Rotation, and Uplift of the Tongbai-Dabie Shan belt in east China. *Geol* 31, 307–310. doi:10.1130/0091-7613(2003)031<0307:mlsler>2.0.co;2

Wang, J. L., Wang, Y., Li, Q., Zheng, D., and Li, D. (2005). Apatite Fission Track Study of Taibai Mountain Uplift in the Mesozoic-Cenozoic. *Nucl. Tech.* 28, 712–716.

Wang, Z. C., Zou, C. N., Tao, S. Z., Li, J., Wang, S. Q., Zhao, C. Y., et al. (2004). Analysis on Tectonic Evolution and Exploration Potential in Dabashan Foreland basin. *Acta Petrolei Sinica* 25, 23–28.

Webb, L. E., Hacker, B. R., Ratschbacher, L., McWilliams, M. O., and Dong, S. (1999). Thermochronologic Constraints on Deformation and Cooling History of High- and Ultrahigh-Pressure Rocks in the Qinling-Dabie Orogen, Eastern China. *Tectonics* 18, 621–638. doi:10.1029/1999tc900012

Xu, H., Liu, S., Qu, G., Li, Y., Sun, G., and Liu, K. (2009). Structural Characteristics and Formation Mechanism in the Micangshan Foreland, south China. *Acta Geol. Sinica* 83, 81–91. doi:10.1111/j.1755-6724.2009.00010.x

Xu, C. H., Zhou, Z. Y., Chang, Y., and Guillot, F. (2010). Genesis of Daba Arcuate Structural Belt Related to Adjacent Basement Upheavals: Constraints from Fission-Track and (U-Th)/He Thermochronology. *Sci China Earth Sci* 53, 1634–1646. doi:10.1007/s11430-010-4112-yL

Yang, Z., Ratschbacher, L., Jonckheere, R., Enkelmann, E., Dong, Y., Shen, C., et al. (2013). Late-stage Foreland Growth of China's Largest Orogens (Qinling, Tibet): Evidence from the Hannan-Micang Crystalline Massifs and the Northern Sichuan Basin, central China. *Lithosphere* 5, 420–437. doi:10.1130/l260.1

Yang, Z., Shen, C., Ratschbacher, L., Enkelmann, E., Jonckheere, R., Wauschkuhn, B., et al. (2017). Sichuan Basin and beyond: Eastward Foreland Growth of the Tibetan Plateau from an Integration of Late Cretaceous-Cenozoic Fission Track and (U-Th)/He Ages of the Eastern Tibetan Plateau, Qinling, and Daba Shan. *J. Geophys. Res. Solid Earth* 122, 4712–4740. doi:10.1002/2016jb013751

Yuan, W. M., Zhang, X. T., Dong, J. Q., Tang, Y. H., Yu, F. S., and Wang, S. C. (2003). A New Vision of the Intracontinental Evolution of the Eastern Kunlun Mountains, Northern Qinghai-Tibet Plateau, China. *Radiat. Measurements* 36, 357–362. doi:10.1016/s1350-4487(03)00151-3

Yuan, W., Carter, A., Dong, J., Bao, Z., An, Y., and Guo, Z. (2006). Mesozoic-Tertiary Exhumation History of the Altai Mountains, Northern Xinjiang, China: New Constraints from Apatite Fission Track Data. *Tectonophysics* 412, 183–193. doi:10.1016/j.tecto.2005.09.007

Yuan, W. M., Du, Y. S., Yang, L. Q., Li, S. R., and Dong, J. (2007). Apatite Fission Track Studies on the Tectonics in Nanmulin Area of Gangdese Terrane, Tibet Plateau. *Acta Petrologica Sinica* 23, 2911–2917.

Yue, G. Y. (1998). Tectonic Characteristics and Tectonic Evolution of Dabashan Orogenic belt and its Foreland basin. *J. Mineralogy Petrol.* (in Chinese) 18, 8–15.

Zhang, G. W., Yu, Z. P., Sun, Y., Cheng, S., Li, T., Xue, F., et al. (1989). The Major Suture Zone of the Qinling Orogenic belt. *J. Southeast Asian Earth Sci.* 3, 63–76.

Zhang, Y. L., Wang, Z. Q., Wang, G., and Wang, K. (2016). Detrital Zircon Geochronology of the Late Paleozoic Taohekou Formation and its Constraints on the Paleozoic Magmatic Events in North Daba Mountains. *Acta Geologica Sinica*. (in Chinese) 90, 728–738.

Zhang, Z. Y., and Dong, S. W. (2009). Superposed Buckle Folding in the Northwestern Daba Mountain, Central China. *Acta Geologica Sinica*. (in Chinese) 83, 923–936. doi:10.1111/j.1755-6724.2009.00008.x

Zhang, Z. Y. (2019). Superposed Buckle Folding at the Upper Structural Levels in Western Dabashan:example from the Jianchi Area in Zhenba County. *Earth Sci. Frontiers*. (in Chinese) 26, 1–15. doi:10.13745/j.esf.sf.2019.3.10

Zheng, D. W., Zhang, P. Z., Wan, J. L., Li, D. M., Wang, F., Yuan, D. Y., et al. (2004). The $^{40}Ar/^{39}Ar$, Fission Track Evidence of Mesozoic Tectonic in Northern Margin of West Qinling Mountain. *Acta Petrologica Sinica* 20, 697–706. doi:10.3321/j.issn:1000-0569.2004.03.034

Zou, X. W., Duan, Q. F., Tang, C. Y., Cao, L., Zhao, W. Q., Wang, L., et al. (2011). SHRIMP Zircon U-Pb Dating and Lithogeochemical Characteristics of Diabase from Zhenping Area in North Daba Mountain. *Geol. China (in Chinese)* 38, 282–291.

Conflict of Interest: Authors TT, JY, ZD, DF and FY are employed by Shaanxi Coal Geology Group Co., Ltd.

The remaining author declares that the research was conducted in the absence of any commercial or financial relationships that could be construed as a potential conflict of interest.